Structure and Function of Cytochrome c_2 in Electron Transfer Complexes with the Photosynthetic Reaction Center of *Rhodobacter sphaeroides*: Optical Linear Dichroism and EPR†

Friedel Drepper* and Paul Mathis

Section de Bioénergétique/DBCM, CEA Saclay, 91191 Gif-sur-Yvette, France

Received June 7, 1996; Revised Manuscript Received October 16, 1996⊗

ABSTRACT: The photosynthetic reaction center (RC) and its secondary electron donor the water-soluble cytochrome (cyt) c_2 from the purple bacterium *Rhodobacter sphaeroides* have been used in cross-linked and non-cross-linked complexes, oriented in compressed gels or partially dried multilayers, to study the respective orientation of the primary donor P (BChl dimer) and of cyt c_2. Three methods were used: (i) Polarized optical absorption spectra at 295 and 10 K were measured and the linear dichroism of the two individual transitions (Q_x, Q_y), which are nearly degenerate within the α-band of reduced cyt c_2, was determined. Attribution of the polarization directions to the molecular axes within the heme plane yielded the average cyt orientation in the complexes. (ii) Time-resolved flash absorption measurements using polarized light allowed determination of the orientation of cyt c_2 in complexes which differ in their kinetics of electron transfer. (iii) EPR spectroscopy of ferricyt c_2 in cross-linked RC−cyt c_2 complexes was used to determine the angle between the heme and the membrane plane. The results suggest the following structural properties for the docking of cyt c_2 to the RC: (i) In cross-linked complexes, the two cytochromes displaying half-lives of 0.7 and 60 μs for electron transfer to P^+ are similarly oriented (difference < 10°). (ii) For cross-linked cyt c_2 the heme plane is parallel to the symmetry axis of the RC (0° ± 10°). Moreover, the Q_y transition, which is assumed to be polarized within the ring III−ring I direction of the heme plane, makes an angle of 56° ± 1° with the symmetry axis. (iii) The dichroism spectrum for the fast phase (0.7 μs) for the non-cross-linked cyt c_2−RC complex suggests an orientation similar to that of cross-linked cyt c_2, but the heme plane is tilted about 20° closer to the membrane. An alternative model is that two or more bound states of cyt c_2 with heme plane tilt angles between 0° and 30° allow the fast electron transfer. Zero-length cross-linking of cyt c_2 may take place in one of these bound states. These orientations of cyt c_2 are compared to different structural models of RC−cyt c_2 complexes proposed previously. The relation of the two kinetic phases observed in cross-linked cyt c_2 complexes to biphasic kinetics of the mobile reaction partners is discussed with respect to the dynamic electrostatic interactions during the formation of a docking complex and its dissociation. A mechanism is proposed in which a pre-orientation of cyt c_2 relative to the membrane plane occurs by interaction of its strong electrostatic dipole with the negative surface charges of the RC. The optimal matching of the oppositely charged surfaces of the two proteins necessitates further rotation of the cyt around its dipole axis.

The electron donation from water-soluble cytochrome (cyt)[1] c_2 to the photosynthetic reaction center (RC) from *Rhodobacter* (*Rb.*) *sphaeroides* provides a useful experimental system to study interprotein electron transfer reactions [for reviews see McLendon and Hake (1992), Moser *et al.* (1995), and Curry *et al.* (1995)]. Two major questions currently under investigation are (i) what are the mechanisms responsible for the formation of transient, functional protein−protein complexes [see, e.g., Tiede *et al.* (1993)] and (ii) which structural properties of the temporary complex are needed in order to achieve fast long-range electron transfer between the redox cofactors buried within the two proteins [see, e.g., Aquino *et al.* (1995)].

The RC from *Rb. sphaeroides* is a membrane integral protein consisting of the three polypeptide subunits L, M, and H (Feher & Okamura, 1978). The X-ray crystallographic structure (Allen *et al.*, 1987a,b; Chang *et al.*, 1991; Chirino *et al.*, 1994; Ermler *et al.*, 1994) reveals that the cofactors are arranged in pairs, bound to the L and M subunit of the RC, along a pseudo-C_2 symmetry axis normal to the membrane. Upon light-excitation of its primary donor (P), a dimer of two excitonically interacting bacteriochlorophyll (BChl) *a* molecules, a cation free radical (P^+) is formed and the electron is transferred through the L-branch of the pigments via a monomeric BChl and a bacteriopheophytin (BPheo) to a first quinone acceptor (Q_A) within 200 ps. This primary charge separation in the cyclic electron transport chain is stabilized on the periplasmic side as P^+ is re-reduced by the secondary electron donor, a soluble monoheme cytochrome c_2 [for reviews see Tiede and Dutton (1993) and Mathis (1994)], and on the cytoplasmic side by electron transfer to the secondary quinone acceptor (Q_B).

† This work was supported by a postdoctoral fellowship from the European Community to F.D.

* To whom correspondence should be addressed. Present address: Institut für Biologie II, Universität Freiburg, Schänzlestr. 1, D-79104 Freiburg, Germany. FAX: +49 761 203 2601. E-mail: drepper@ruf.uni-freiburg.de.

⊗ Abstract published in *Advance ACS Abstracts,* January 1, 1997.

[1] Abbreviations: cyt, cytochrome; RC, reaction center(s); BChl, bacteriochlorophyll; BPheo, bacteriopheophytin; P, reaction center primary donor; *Rb.*, *Rhodobacter*; *Rps.*, *Rhodopseudomonas*; Δ*A*, absorption change; EPR, electron paramagnetic resonance.

S0006-2960(96)01351-7 CCC: $14.00

The bacterial cytochromes c_2 and the eucaryotic cytochromes *c* are small (12−14 kDa) single-heme proteins performing analogous functions as mobile electron carriers between membrane-bound enzymes in photosynthetic and respiratory electron transport chains, respectively [for reviews, see Moore and Pettigrew (1990) and Caffrey and Cusanovich (1994)]. For both proteins, the interaction with their physiological reaction partners is predominantly electrostatic, involving as "interaction domain" the positively charged residues surrounding the solvent-exposed heme edge (Okamura & Feher, 1983; Margoliash & Bosshard, 1983; Hall *et al.*, 1987a,b; Long *et al.*, 1989). For an efficient association reaction, their electrostatic dipole is proposed to be important in order to pre-orient the cytochrome as it approaches its reaction partner (Koppenol & Margoliash, 1982; Margoliash & Bosshard, 1983; Northrup *et al.*, 1987; Tiede *et al.*, 1993).

Photosynthetic RC provide unique opportunities for studying the details of the protein−protein interactions and the electron transfer reactions of cytochromes *c*, because single turnover kinetics can be measured following excitation of the RC by short flashes [for more details on kinetic studies, see preceding paper (Drepper *et al*., 1997)]. The precise binding site on the RC, the orientation of cyt c_2 within the temporarily formed complex, and whether cyt c_2 is bound in various orientations, are controversial. For the electrostatic RC−cyt c_2 complex, three different structures have been modeled based on the maximization of the number of charge pairs between the positively charged cyt interaction domain and negative charges on the periplasmic RC surface. In the first model, using the three-dimensional structure of *Rhodospirillum rubrum* cyt c_2, the cyt was positioned nearly symmetrically over the primary donor (Allen *et al.*, 1987b). However, this position is rendered unlikely by the results of a recent mutagenesis study probing the importance of single symmetry-related amino acids at the RC surface for the binding affinity of the cyt (Rongey *et al.*, 1994; Adir *et al.*, 1996). In the second model, accomodating the results of a previous linear dichroism study for the orientation of cyt c_2 (Tiede, 1987), the cyt was shifted toward the M side of the RC surface (Tiede & Chang, 1988). More recently, co-crystals of the RC and cyt c_2 have been obtained and the X-ray diffraction data set to 4.5 Å resolution was used to model the structure of cyt c_2 (Axelrod *et al.*, 1994) in the electron density map (Adir *et al.*, 1994, 1996). One unique docking position is proposed in that study which differs from the model proposed by Tiede and Chang (1988) in the following aspects. The cyt c_2 is shifted even more toward the M side of the RC and rotated by about 90° around the symmetry axis of the RC. As to the orientation of the heme relative to the membrane plane, the two models differ in a rotation by 35° approximately around the heme plane normal (Tiede & Chang, 1988; Adir *et al.*, 1996; coordinates kindly provided by H. Axelrod and G. Feher). Whereas in the Tiede and Chang model both rings II (exposed heme edge with thiol bridge to Cys 18) and III (exposed propionate) are in close approach to the RC surface, the co-crystal model orients the heme molecular *x*-axis almost perpendicular to the membrane plane with ring II pointing precisely to the RC surface. The observed fast electron transfer in the co-crystal indicated that the proposed cyt position could correspond to that in solution. The reason for the discrepancy between the cyt orientation in the model for cyt c_2 in the co-crystals and that derived from the linear dichroism data is not clear. Furthermore, some important parameters for the electron transfer reaction are controversial, such as the heme to P distance or a possible role of specific amino acids in the electron transfer pathway (Wachtveitl *et al.*, 1993; Aquino *et al.*, 1995; Adir *et al.*, 1996).

For the association of cytochromes *c* and c_2 with their reaction partners, an alternative mechanism has been proposed that involves primarily the interaction of delocalized electrostatic domains of the proteins and not specific salt-bridges between charged residues (McLendon, 1991; Tiede *et al.*, 1993). Such a mechanism could result in various cyt orientations, a subpopulation of which may be more competent in electron transfer. However, in the case of the interaction between cyt c_2 and the RC, the observed distinct kinetic phases of P^+ reduction by cyt c_2 (see also preceding paper) indicate rather specific electron transfer complexes. Thus, unanswered questions are how specific is the temporary complex and how is this specificity achieved during the docking process.

As shown in the preceding paper, a cross-linked RC−cyt c_2 complex has functional properties similar to the spontaneously formed complex. Here, we reinvestigated structural properties of the docking of cyt c_2 to the RC, in the covalent as well as in noncovalent complexes. Using RC oriented in compressed polyacrylamide gels in combination with linear dichroism spectroscopy, we measured the orientation of optical transition moments of the heme which allow to determine the orientation of cyt c_2 relative to the symmetry axis of the RC. The dichroism of optical transitions of pigments in the RC, for which the polarization directions are known relative to the C_2 symmetry axis are used as references. The discrepancies between cyt orientations in previous models of RC−cyt c_2 complexes (see above) prompted us to study specifically the orientation of cyt c_2 in parallel with its electron transfer kinetics by using time resolved polarized absorption spectroscopy. In order to improve the quantitative reliability of the linear dichroism data, low-temperature linear dichroism spectra were recorded to improve the spectral resolution of optical transitions, and complementary information on the cyt orientation was obtained by using EPR spectroscopy.

EXPERIMENTAL PROCEDURES

Chemicals. Phosphatidylcholine was isolated from egg yolk by the method of Singleton *et al.* (1965). Egg yolk phosphatidic acid was obtained from Avanti Polar Lipids. Other chemicals were purchased from Sigma.

Preparation of Materials. Reaction centers from *Rb. sphaeroides* R26 were isolated as described by Feher and Okamura (1978). This carotenoid-less strain was used in the present study instead of the wild type (2.4.1) used in the preceding article in order to facilitate the analysis of optical spectra in the 500−600 nm region. Cyt c_2 was isolated as described in the preceding article. Cross-linking of cyt c_2 with the RC was carried out by using *N*-hydroxysulfosuccinimide (NHS) and 1-ethyl-3-(3-dimethylaminopropyl)-carbodiimide (EDC) essentially as described for the wild type RC (see preceding article) except that for the buffer exchange following the incubation with cross-linker, 0.1% sodium cholate was used instead of LDAO. RC or RC−cyt c_2 complexes were reconstituted in lipid vesicles essentially

according to the procedure described by Richard *et al.* (1995). Phosphatidylcholine and phosphatidic acid were used at a ratio of 9:1. The initial protein to lipid to cholate ratio (w/w) was 1:10:20. The cholate was removed by using Bio-Beads SM-2 (Bio-Rad) in three successive incubations for 20 min to 1 h on ice. Vesicles were sonicated immediately before use for approximately 1 min.

Preparation of Oriented Membranes. Reconstituted RC vesicles were included in polyacrylamide gels immediately before polymerization. Membrane orientation was induced by uniaxial squeezing of the gels to about 70% of their initial length (Abdourakhmanov *et al.*, 1979). Aqueous polyacrylamide gels were prepared as described by Tiede (1987) with minor modifications. The gel-forming mixture contained final concentrations of 9% acrylamide, 0.3% bisacrylamide, 0.24% tetramethylethylenediamine, 0.1% ammonium persulfate, and 10 mM Tris, pH 7.8. RC vesicles and soluble cyt c_2 (30 μM) or vesicles containing RC−cyt c_2 complexes were added to the mixture at a final RC concentration of ~1 μM. The gels were polymerized within a few minutes at about 20 °C under running water. Gels were then incubated in the dark at 4 °C for at least 3 h in 10 mM Tris, pH 7.8, 1 mM sodium ascorbate, 50 μM *N*,*N*′,*N*′,*N*′-tetramethyl-*p*-phenylenediamine, and 50 μM 1,4-naphthoquinone. For gels containing soluble cyt c_2, this protein was also added to the incubation medium at the same concentration as in the gel. For low-temperature experiments, 60% glycerol (v/v) was added to the gel-forming mixture and to the incubation medium, and gels were incubated overnight. Spectra of the RC−cyt c_2 complex with oxidized cyt were taken after incubation overnight in a mixture of 2:1 of potassium ferri- and ferrocyanide with a total concentration of 10 mM. These conditions poise the ambient redox potential to approximately 425 mV (O'Reilly, 1973). Sections of 2.5 cm of the gels were placed in a standard 1 cm × 1 cm path length plastic cuvette and compressed along the vertical direction of the cuvette.

Oriented membranes for EPR measurements were prepared by using the technique of Blasie *et al.* (1978). RC−cyt c_2 complexes reconstituted in lipid vesicles were spread on stripes of mylar film and then partially dried in 90% humidity atmosphere under argon in the dark at 4 °C for approximately 24 h. Four to six stripes were piled up into an EPR tube. Room light intensities during the preparation of the reconstituted RC−cyt complexes were sufficient to oxidize the cyt c_2 almost completely.

EPR Spectroscopy. EPR spectra were recorded by using a Bruker 300 X-band spectrometer fitted with an Oxford Instruments cryostat and temperature control system. The tube was rotated manually in order to change the orientation of the multilayers relative to the magnetic field and the angles were read on an angular scale connected to the cavity housing.

Kinetic Measurements. Flash-induced absorbance changes were measured with a single-beam spectrophotometer. The measuring light from a 100 W tungsten−halogen lamp was selected by narrow-band interference filters and was shielded from the sample by a photoshutter until 5 ms before the measurement. The detecting silicon photodiode (1 cm^2) was protected by an interference filter (2.6 nm FWHM) and a Corning 4/96 blue-green glass filter or Schott RG 780/3 for measurements in the green spectral region and at 870 nm, respectively. The output of the photodiode was amplified with an electrical bandwidth ranging from dc to 1 MHz with dc offset compensation. Flash excitation was provided by a dye laser (700 nm) pumped by a frequency-doubled Nd:YAG laser (5 ns FWHM). In some of the experiments it was replaced by a ruby laser (695 nm, 25 ns FWHM). In all experiments, flashes of near-saturating intensity were used. The time interval for dark adaptation of the sample between successive flashes was 7.5 or 60 s for experiments using cross-linked or soluble cyt c_2, respectively, which was chosen to be sufficiently long to allow a complete return to equilibrium. Kinetics of absorption changes were recorded with a Nicolet digitizer. Ten to 20 individual signals were averaged for the kinetic traces used in the analysis.

Analysis of Kinetic Measurements. A sum of two or three single-exponential components was determined as the least-squares fit to the measured absorbance transients using Marquardt's algorithm. In general, the amplitudes and rates were allowed to vary during the fitting procedure without restriction. However, for analysis of transients measured with polarized light the value of the half-life of the fast component was kept constant for wavelengths where the small amplitude of this component prevented a determination of its half-life. In these cases the value of the half-life determined with unpolarized light was used.

Linear Dichroism Measurements. Polarized absorption spectra were recorded on a Cary 5E spectrophotometer. A Nicol prism polarizer placed in the beam before the sample was used to provide polarized measuring light. The direction of polarization was changed by rotating the prism and baselines were recorded for each position separately. For some of the measurements in the green spectral region a polarizing filter (Polaroid HN38) was used instead of the prism polarizer. This setup provided a comparable degree of polarisation and about 10% less transmission compared to the prism polarizer. When spectra for one sample were recorded with both methods, virtually identical results were obtained. For measurements of polarized flash-induced absorbance changes, the same polarizers as described above were used and placed in the measuring light beam before the sample. All measurements with polarized light were repeated in reverse order of the polarization directions to check for any progressive changes of the sample. Such effects were not observed, however. Low-temperature absorption and linear dichroism spectra were recorded with an apparatus described previously (Breton, 1985).

Analysis of Linear Dichroism Measurements. The squeezing of polyacrylamide gels produces a uniaxial orientation for the membrane proteins with the membrane normal parallel to the direction of compression (Abdourakhmanov *et al.*, 1979; Breton, 1985). This direction will be referred to as *vertical* (V) whereas the *horizontal* (H) directions lie in the membrane plane. The measured linear dichroism can be expressed by a parameter S (often named anisotropy or order parameter):

$$S = (A_V - A_H)/3\bar{A} \qquad (1)$$

where A_V and A_H denote the absorption for light polarized parallel or perpendicular to the direction of uniaxial orientation (Tiede, 1987). $\bar{A}$ is the absorption of the pigments in an unoriented sample; in our case, it can be obtained from polarized spectra of the oriented sample by the following

relationship (Hofrichter & Eaton, 1976):

$$\bar{A} = (A_V + 2A_H)/3 \quad (2)$$

When light-induced absorbance changes were measured, A_V, A_H, and $\bar{A}$ were simply replaced by ΔA_V, ΔA_H, and $\Delta\bar{A}$, respectively. For a single linearly polarized transition moment in a perfect uniaxial symmetry, its angle θ relative to the direction of uniaxial orientation is related to the parameter S as follows (Hofrichter & Eaton, 1976):

$$S = \frac{3\cos^2\theta - 1}{2} \quad (3)$$

In practice the molecules are not perfectly oriented. A simple model for the quantitative treatment of imperfect orientation has been used by Rafferty and Clayton (1979). They assumed a fraction, f, of molecules with perfect uniaxial orientation and a fraction $(1 - f)$ of molecules that are randomly oriented. In this case, assuming a homogeneous extent of orientation throughout the sample, the basic equations for the absorption for vertically and horizontally polarized light (Hofrichter & Eaton, 1976) take the following form:

$$A_V = 3f\bar{A}\cos^2\theta + (1 - f)\bar{A}$$
$$A_H = {}^3/_2 f\bar{A}\sin^2\theta + (1 - f)\bar{A} \quad (4)$$

Substitution of A_V and A_H in eq 1 and comparison with eq 3 yields:

$$S = fS_T \quad (5)$$

giving a simple relation between the linear dichroism S_T for the transition that would result from a perfectly oriented sample and the observable linear dichroism in the partially oriented sample. Other deviations from a perfect orientation could be, for example, an angular distribution for the membranes or a non-zero angle between the membrane normal and the direction of compression. It is of note, however, that the quantitative treatment of these two cases has led to approximative expressions of the same factorized form as eq 5 (Rothschild & Clark, 1979; Michel-Villaz *et al.*, 1979; Nabedryk & Breton, 1981; van Amerongen & Struve, 1995).

The extent of orientation of the RC in squeezed polyacrylamide gels was determined from light-induced absorbance changes at 870 nm, due to oxidation of P, using polarized measuring light. The 870 nm band has been attributed to the lower exciton transition of the two special pair BChl monomer Q_y transitions (Verméglio & Clayton, 1976). We assume this transition to be polarized parallel to the membrane plane, i.e., $\theta = 90°$ and $S_T = -0.5$ (Rafferty & Clayton, 1979; Breton, 1988; see also Discussion). The low-temperature linear dichroism spectra were calibrated by using the Q_x bands of the two bacteriopheophytins at 532 nm ($BPheo_L$) and 545 nm ($BPheo_M$) [see Breton *et al.* (1989)] as internal reference for the recorded spectrum. Their theoretical order parameter S_T was calculated from the orientation of the molecular x-directions, 77° ($BPheo_L$) and 80° ($BPheo_M$) relative to the RC symmetry axis, which were determined from the atomic structure of the RC (Ermler *et al.*, 1994). From the observed linear dichroism for the bands at 532 and 545 nm, the calibration factor for the linear dichroism spectra was calculated according to eq 5. In this case, the calibration factor included both apparatus parameters (Breton, 1985) and the extent of orientation of the RC. A confidence interval of approximately 10% was estimated for the calibration factor assuming an uncertainty of ±5° for the Q_y transitions within the BPheo plane. It is of note that at the extreme angles of 90° and 0° slight deviations in θ yield very small errors in S_T due to a first derivative of the $S(\theta)$ dependence (eq 3) close to zero. On the other hand, determination of the angle for an optical transition has its highest precision at intermediate angles where experimental errors in S as well as the error in f introduce little error in θ.

The α-band of mitochondrial cyt *c* (Eaton & Hochstrasser, 1967; Verméglio *et al.*, 1980) and cyt c_2 (Tiede, 1987) consists of two nearly degenerate linear transitions that are assumed to be polarized within the heme plane and orthogonal to each other. For cyt c_2 the line positions of the two transitions differ by approximately 3 nm [see Tiede (1987)]. In the present work the dichroism for the two individual transitions was quantitatively analyzed by fitting a sum of theoretical line shapes to the room- and low-temperature absorption spectra using the program Spectracalc (Galactic). Accurate fits to the experimental spectra were obtained using mixed, 50% Lorentzian and 50% Gaussian, line shapes for the individual transitions of the α-band. This ratio was used throughout the curve-fitting analysis. First the line position, line width, and height for the Q_x and Q_y transitions were determined from the fit to the absorption spectra. For the fit to the linear dichroism spectra, the line positions and line widths were kept fixed at the values determined for the absorption spectrum. For room-temperature spectra, the line positions were additionally assumed to be separated by the same wavelength difference as that observed at low temperature. Confidence intervals for the intensities obtained from the fits were estimated by systematic variation of the restrained parameters, i.e., the ratio Lorentzian vs Gaussian line shape or the peak positions for the room temperature spectra.

RESULTS

Linear Dichroism of cyt c_2 Absorbance Changes. Flash-induced absorbance changes using linearly polarized light were measured on oriented RC with cross-linked or soluble cyt c_2. The results with cross-linked cyt c_2 will be presented first and then serve as a reference for those obtained with soluble cyt c_2. Figure 1 (panel a) shows absorbance changes at 870 nm of RC that are oriented in squeezed polyacrylamide gels with cross-linked cyt c_2 oxidized prior to the excitation; these conditions were obtained without addition, i.e., before any incubation of the gels with ascorbate and redox mediators. The absorption transients were measured with light polarized parallel (left, ΔA_V) or perpendicular (right, ΔA_H) to the gel squeezing direction (which was vertical in the measuring beam). The absorbance change at 870 nm associated with the formation of P^+ by the flash-excitation shows the largest amplitude when measured with horizontally polarized light (Figure 1a, right trace). In panel b of Figure 1, absorbance changes at 600 nm are shown for a sample in which cyt c_2 is poised reduced before the excitation. The initial bleaching at 600 nm again shows a strong dichroism, but with the largest amplitude for vertically polarized light.

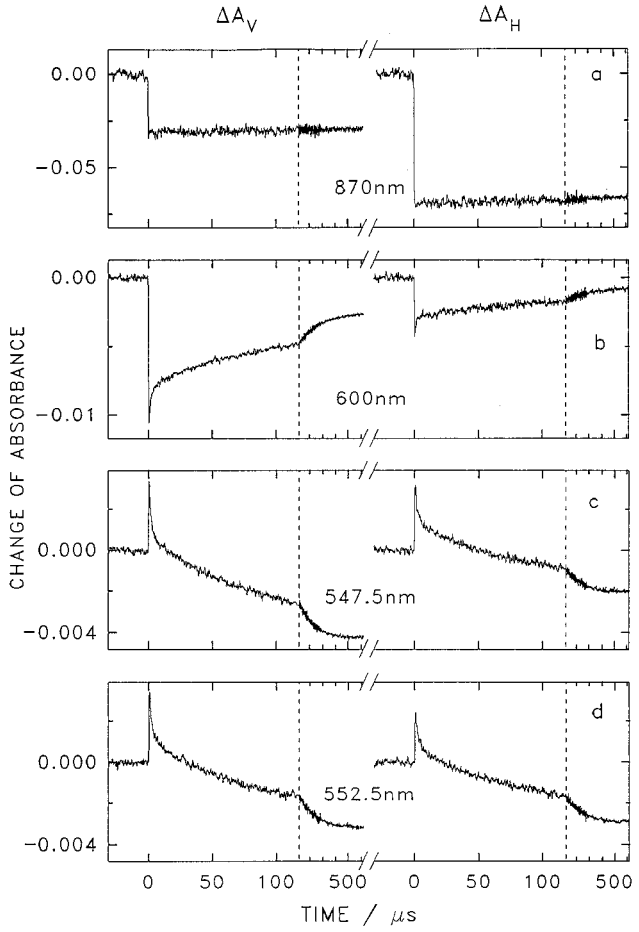

FIGURE 1: Absorbance changes induced by a laser flash for cross-linked RC−cyt c_2 complexes in proteoliposomes oriented in squeezed polyacrylamide gels. Gels contained RC from *Rb. sphaeroides* R26 at a concentration of about 1 μM. The measuring light of the indicated wavelengths was polarized vertically (left traces, ΔA_V) or horizontally (right traces, ΔA_H) relative to the membrane plane (orthogonal to the direction of compression). Traces were recorded before (a) or after reducing cyt c_2 by incubation of the gels as described in Experimental Procedures (b−d). The vertical dashed lines correspond to a 10-fold time scale expansion.

The polarized absorbance changes of flash-induced bleaching in the Q_x (600 nm) and Q_y (870 nm) bands of P will be used for a quantitation of the extent of orientation of the RC (see below).

When cyt c_2 is reduced before the excitation, the subsequent fast kinetics of re-reduction of P^+ monitor the electron donation from cyt c_2. The kinetics of absorption transients at 600 and 870 nm measured under these conditions were similar to the measurements in the P^+ absorption band at 1283 nm (see preceding article), showing a fast and an intermediate kinetic phase with half-lives of about 1.2 ± 0.2 μs and 70 ± 10 μs, and a very slow phase decaying in the ms time domain. The relative amplitudes for the fast and the intermediate phase of 0.30 and 0.40, respectively, which are similar to those measured for this type of RC−cyt c_2 complexes in solution, are attributed to a reduction of P^+ by cross-linked cyt c_2. The ms phase is attributed to a reduction of P^+ by the redox mediator or by back-reaction from acceptor side quinones. A slightly smaller amplitude of the fast phase was found in this work where we used the RC from *Rb. sphaeroides* R26 compared to that of 0.40 obtained with the wild type (2.4.1) RC using the same protocol for the cross-linking with cyt c_2 (see preceding article). The difference between the half-life of the fast phase in the present kinetic measurements and that of 0.7 μs observed at 1283 nm for the cross-linked complex in solution was found to originate from the limiting instrument response time. Identical half-lives were observed for the RC−cyt c_2 complex in gels or in solution when detecting with a non-limiting time response. A slower time response has been accepted in the present measurements in order to benefit from a much better signal to noise ratio obtained with a 1-MHz bandwidth amplifier.

At 547.5 and 552.5 nm (Figure 1, panels c and d), the immediate absorption increase associated with the formation of P^+ is followed by a decay which includes the two kinetic phases observed at 600 nm. This decay is attributed to the reduction of P^+ and to a negative contribution due to the oxidation of cyt c_2. The absorbance change at 547.5 nm shows almost no linear dichroism for the initial (positive) amplitude due to formation of P^+. However, both kinetic phases of the subsequent oxidation of cyt c_2 have the largest amplitude with vertically polarized light. For both kinetic phases the difference between ΔA_V and ΔA_H is significantly smaller at 552.5 nm (panel d). It is of note that the initial absorbance change due to P^+ formation shows a larger linear dichroism compared to that at 547.5 nm.

Curve-fitting of a sum of two exponentials to the signals shown in Figure 1 allows determination of the amplitude of the initial absorbance change induced by the laser flash that is attributed to the photooxidation of P as well as amplitudes for the fast and the intermediate kinetic phases of P^+ reduction. The linear dichroism for the amplitude of the initial photooxidation of P is close to zero between 535 and 550 nm whereas it increases rather sharply between 550 and 565 nm to about +0.4 ($\Delta LD/\Delta A$) at 565 nm (see Figure 2D). Consequently, the partial absorbance change due to reduction of P^+ in the two kinetic phases contributes also to the observed linear dichroism. For each kinetic trace, the amplitude of the absorbance change due to the formation of total P^+ is given by the initial amplitude immediately after the flash and, furthermore, the contribution of P^+ reduction in each of the two subsequent kinetic phases can be determined from their amplitude ratio at 600 nm, i.e., 30% for the fast phase and 40% for the intermediate phase. From the amplitude of the fast and the intermediate phases, we then subtracted 30% and 40% of the initial signal in order to obtain the absorbance changes due to the two phases of cyt c_2 oxidation.

The net absorbance changes and linear dichroism associated with oxidation of cross-linked cyt c_2 are shown in Figure 2 (A and B) for the fast (closed circles) and the intermediate phase (open squares), in the studied wavelength region (535−565 nm). The data are normalized to the maximum of the absorption change at 550 nm (Figure 2A). The absorbance and linear dichroism chemically reduced minus oxidized difference spectra for oriented RC with cross-linked cyt c_2 are shown by the solid lines. Figure 2A shows that the difference spectra are the same for the two kinetic phases and also for the chemically reduced minus oxidized conditions. Furthermore, Figure 2B shows that the linear dichroism difference spectrum obtained by chemical reduction and oxidation can account for the average dichroism of the flash-induced absorbance changes of the two kinetic phases associated with the oxidation of cyt c_2. Further minor

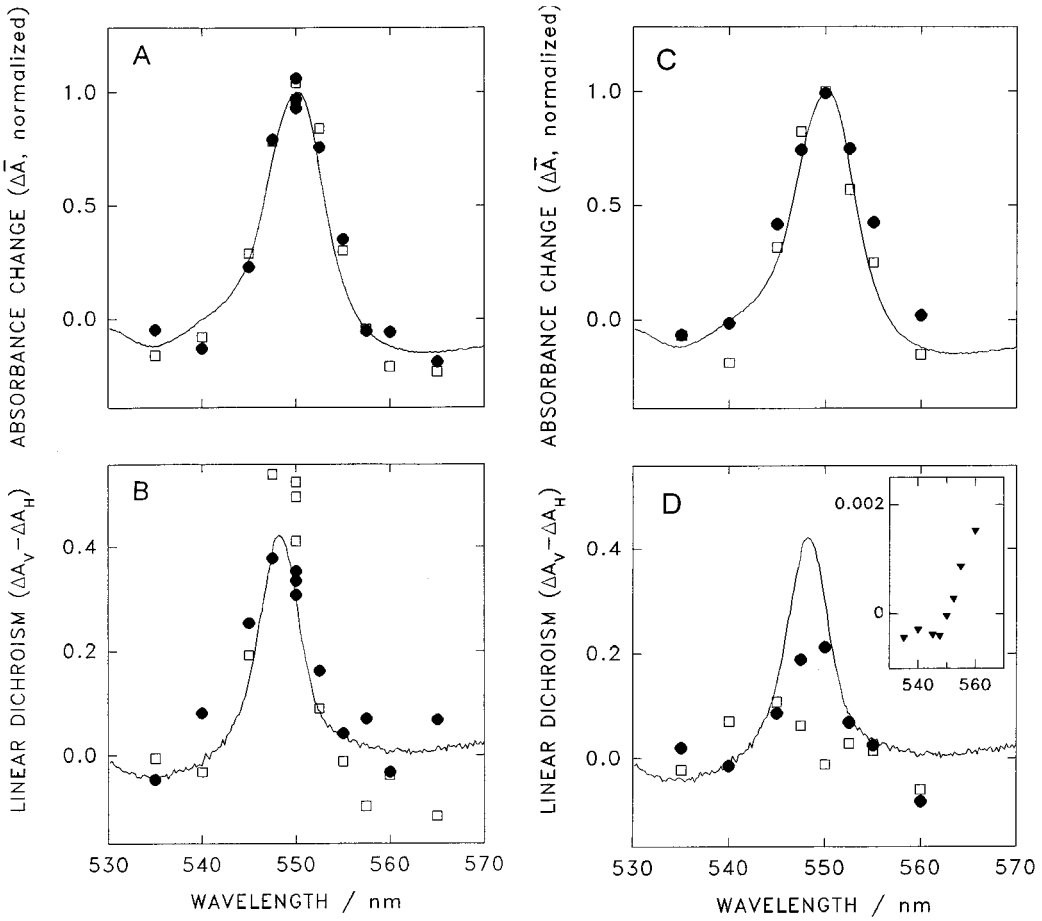

FIGURE 2: Absorbance changes (A and C) and linear dichroism (B and D) of cyt c_2 cross-linked (A and B) or spontaneously bound (C and D) to the RC and oriented in squeezed polyacrylamide gels. Amplitudes for the fast (●) and the intermediate kinetic phase (□) were corrected for the absorbance change due to reduction of P^+ as described in the text. The data in A and C are normalized to the maximum of the absorption spectrum at 550 nm. The solid lines give chemically reduced minus oxidized difference spectra of cross-linked cyt c_2. The absorption spectrum has been set to zero at the average value of the three isosbestic points 528.4, 540.9, and 555.9 nm and normalized to 1 at 550 nm. The linear dichroism data are given in the normalized units. The linear dichroism ($\Delta A_V - \Delta A_H$) for the initial amplitude of flash-induced absorbance changes due to formation of P^+ is shown in the inset of D.

differences in the spectra will be discussed below.

Similar measurements as shown in Figure 1 were carried out using oriented RC in the presence of 30 μM soluble cyt c_2 (data not shown). The linear dichroism for the initial amplitudes at 600 and 870 nm was the same as observed with cross-linked RC−cyt c_2 complexes within measuring accuracy. The time-resolved P^+ re-reduction showed two dominant kinetic phases with half-lives of 1.2 ± 0.2 μs and 50 ± 15 μs and relative amplitudes of 0.34 and about 0.35, respectively. About one-third of P^+ decayed more slowly with multiple half-lives between 0.2 and 2 ms. It is attributed to RC that are less accessible to cyt c_2 and are in part reduced by the redox mediator. The curve fitting of the absorbance transients and the deconvolution of contributions from re-reduction of P^+ were carried out similarly as described above for cross-linked cyt c_2. Figure 2C presents the amplitudes of the fast (closed circles) and the intermediate component (open squares) for the absorbance changes due to oxidation of cyt c_2. Figure 2D shows the linear dichroism for the amplitudes of the two kinetic phases relative to the normalized absorbance changes given in Figure 2C. For comparison the chemically reduced minus oxidized difference spectra for cross-linked cyt c_2 are redrawn from Figure 2A and B. The linear dichroism spectrum of the fast phase (Figure 2D, closed circles) is similar to that observed for the equivalent kinetic phase in the cross-linked complex (Figure 2B), with a smaller maximum value. For the intermediate phase, no linear dichroism could be observed (Figure 2D, open squares). This absence of linear dichroism supports the conclusion, already reached in the preceding article, that this intermediate phase is of different origin as the 60-μs phase obtained in cross-linked complexes.

Extent of Orientation of Reaction Centers in Squeezed Polyacrylamide Gels. The flash-induced absorbance changes measured with polarized light at 870 nm were used for a quantitative determination of the extent of orientation of the reaction centers. The observed linear dichroism at 600 and 870 nm was the same for RC and RC−cyt c_2 complexes within the experimental variation between individual experiments. For the flash-induced absorbance changes at 870 nm a linear dichroism $(A_V - A_H)/\bar{A}$ of -0.72 ± 0.05 was determined in four independent measurements with RC and cross-linked RC−cyt c_2 complexes, corresponding to a value S of -0.24 ± 0.017. Assuming the lower excitonic transition of the special pair to lie parallel to the membrane ($\theta = 90°$, $S_T = -0.5$, see Experimental Procedures) we obtain a value of $f = 0.48 \pm 0.03$ for the extent of orientation of RC in the polyacrylamide gels (*cf.* eq 5). From the absorbance changes at 600 nm a linear dichroism $(A_V - A_H)/\bar{A}$ of 1.25 ± 0.1 was determined, corresponding to a value of 0.42 ± 0.03 for the parameter S. Using the value of f determined above,

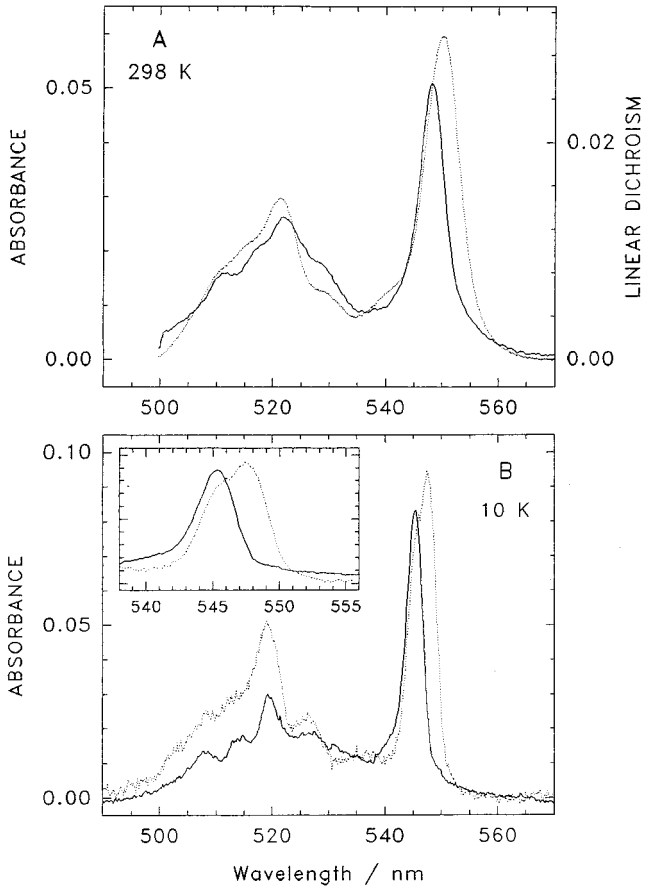

FIGURE 3: Absorption (dashed line) and linear dichroism spectra (solid line) of reduced cyt c_2 cross-linked to the RC. Spectra of the RC without cytochrome recorded under the same conditions were subtracted after normalization at 600 nm. (A) Spectra recorded at 295 K on proteoliposomes (RC concentration about 3 μM) that were oriented in aqueous polyacrylamide gels. (B) Spectra at 10 K measured on similar samples oriented in gels containing 60% (v/v) glycerol. In the inset, the α-band region of the spectra is shown enlarged. In A and B, corrected linear dichroism spectra corresponding to a perfect uniaxial orientation are shown on the same scale as the absorption spectra (left vertical axes). For A, the original scale for the linear dichroism spectrum is also given (right vertical axis).

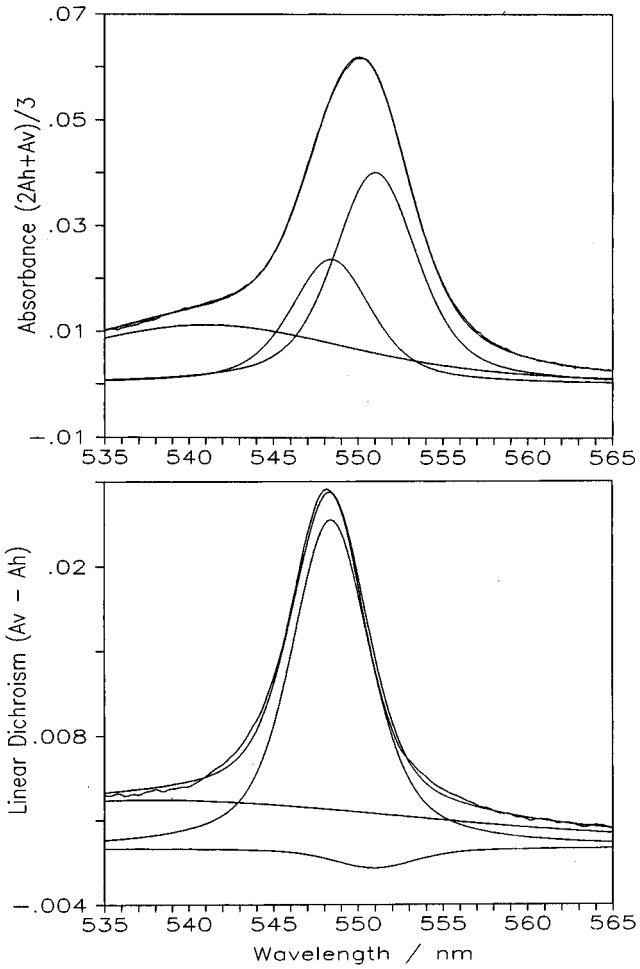

FIGURE 4: α-Band region of the absorption (A, top) and linear dichroism spectra (B, bottom) of reduced cyt c_2 cross-linked to the RC at 295 K (data redrawn from Figure 3A). The fits of the sum of three Lorentzian line shapes to the data as well as the individual transitions, two non-degenerate α-band transitions, and a minor component from the adjacent β-band, are also shown (see text for more explanation).

we calculate a parameter S_T for the 600 nm Q_x transition of 0.875 ± 0.125, yielding an angle relative to the C_2 axis of $\theta = 17°$ with lower and upper limits of 0° and 24°, respectively.

Linear Dichroism for the α-Band Transitions of cyt c_2. Spectra from oriented RC with and without cross-linked cyt c_2 were recorded under identical conditions and subtracted after normalization at 600 nm. Figure 3 shows the resulting absorption and linear dichroism spectra of cross-linked cyt c_2 recorded at room temperature (A) and at 10 K (B). At both temperatures the linear dichroism spectrum shows an α-band peak which has about 65% of the width of the absorption spectrum and a maximum blue-shifted by about 2 nm. At 10 K the contributions of two individual transitions to the α-band are already visible in the absorption spectrum (see Figure 3B, inset).

In order to determine the orientation of the Q_x and Q_y transitions of cyt c_2, the α-bands of the spectra were fitted by a sum of two Lorentzian−Gaussian mixed line shapes as described in the Experimental Procedures. A minor contribution from the adjacent β-band to the spectra had to be included as a third transition (541 nm at 295 K) in order to obtain accurate fits to the data. The large width (23 nm) and the small amplitude of this transition precluded a further line shape and orientation analysis for this band. Its line shape may also be slightly distorted due to an inclined baseline in the linear dichroism spectra. The fits for the room-temperature absorption and linear dichroism spectra are shown in Figure 4A and B, respectively. The line shape parameters obtained for the room-temperature and the 10 K spectra are summarized in Table 1. The intensities for individual transitions are given relative to the total area of the three bands used in the fit of the absorption spectrum. Whereas for the 295 K spectra the extent of sample orientation is accounted for when S_T is calculated from eq 5 using $f = 0.49$, for the 10 K spectra this correction is included in the calibration of the spectra by using internal reference bands (see Experimental Procedures). The resulting angles for the Q_x and Q_y transition relative to the normal to the membrane plane are given in the last column of Table 1. The highest precision is obtained for the orientation of the Q_y transition yielding $\theta = 56° \pm 1°$. Assuming that the two transitions are polarized within the heme plane and are orthogonal to each other, the possible orientations of Q_x are restricted to angles $\theta \geq 33°$. From the angles that each of the two transitions makes with the membrane normal the

Table 1: Orientation Analysis of Heme Q_x and Q_y Transitions in Cross-Linked RC−cyt c_2 Complexes in Squeezed Polyacrylamide Gels

				intensity[b]			
transition	T (K)	maximum (nm)	width[a] (nm)	abs[c]	LD[d]	S_T[e]	θ (deg)[f]
Q_x	10	545.3	3.9	0.35	0.59 ± 0.09	0.56 ± 0.14	32.8 ± 6
	295	548.4	6.2	0.26	0.25 ± 0.015	0.32 ± 0.05	28.2 ± 7
Q_y	10	547.9	3.4	0.51	-0.05 ± 0.04	-0.03 ± 0.025	56 ± 1
	295	551.0	6.6	0.45	-0.015 ± 0.015	-0.01 ± 0.012	55.7 ± 1

[a] Full width at half-maximum. [b] Relative area under transition curve (sum of intensities for the three transitions in the absorption spectrum set to 1.0). [c] Estimated error ±10%. [d] $A_V - A_H$. For 10 K spectra, the calibration using internal reference bands also accounts for imperfect sample orientation (see Experimental Procedures). [e] Calculated using eqs 1 and 5. For 295 K data, a value of $f = 0.48 \pm 0.03$ for the extent of sample orientation has been used. [f] Angle between the transition moment and the symmetry axis of the RC. Note that Q_x is further restricted to values $\theta \geq 33°$ by the more accurately determined angle for Q_y and by the assumption of two orthogonal transitions.

angle between the heme plane and the membrane can be calculated from the vector cross product. The resulting heme plane tilt angle is 90° which has, however, a relatively high uncertainty ranging from 72° to 90°.

EPR Spectroscopy of Oriented Multilayers. The *z*-axis of the magnetic susceptibility tensor for cytochrome *c* is within 5° of the normal to the heme plane (Mailer & Taylor, 1972; Taylor, 1977). Therefore, the orientation dependence of the g_z signal is sufficient to determine the tilt angle of the heme plane with respect to the membrane. This is especially helpful as it provides complementary experimental information in addition to optical linear dichroism data. Since the main optical transitions of the porphyrin π-system are polarized within the heme plane, linear dichroism measurements have the highest uncertainty in the heme plane tilt angle.

Isolated ferricyt c_2 in solution has a neutral pH EPR spectrum (data not shown) of the typical low-spin form with principal g values of $g_z = 3.29$, $g_y = 2.06$, and $g_x \approx 1.14$. EPR spectra of cross-linked ferricyt c_2 in multilayers of vesicles containing RC−cyt c_2 complexes are shown in Figure 5 for several orientations (between +90° and −90°) of the multilayers relative to the direction of the magnetic field. The signal at $g = 3.29$ corresponds to the g_z position in the spectrum of isolated cyt c_2. It is maximal at an angle of 0° between the multilayer plane and the direction of the magnetic field. The minimal intensity that corresponds to about 50% of the intensity at 0° is observed for signals recorded at 90°. In the polar plot of Figure 5B the height of the g_z signal after subtraction of the signal at 90° is plotted as a function of the orientation of the multilayer. One single maximum at 0° can be observed, indicating that the axis of the g_z value is oriented parallel to the membrane plane. Similar results were obtained for isolated RC with cross-linked cyt c_2. However, the extent of orientation was lower in that case.

The main g_y signal for the RC-bound cyt c_2 is observed at g values close to the $g_y = 2.06$ of isolated cyt c_2 (not shown in Figure 5A). However, it is barely discernible from a radical signal due to the RC in the $g = 2$ region. Additional signals also appeared between $g = 2.4$ and 2.0, the positions and relative intensities of which varied between individual samples. The most obvious signal is observed at $g = 2.26$. It can also be identified in the spectrum of isolated ferricyt c_2, but it has a very low intensity (not shown). Its intensity was increased for spectra of the RC−cyt c_2 complexes, when studied in solution (not shown) as well as in the partially dried multilayers (Figure 5A). A possible effect of the cross-linking reagents was checked by EPR spectra of cyt c_2 in solution taken either before or after the incubation for cross-linking. No significant differences were observed between these spectra. Evaluation of the orientation dependence of the g_y signals was therefore not possible.

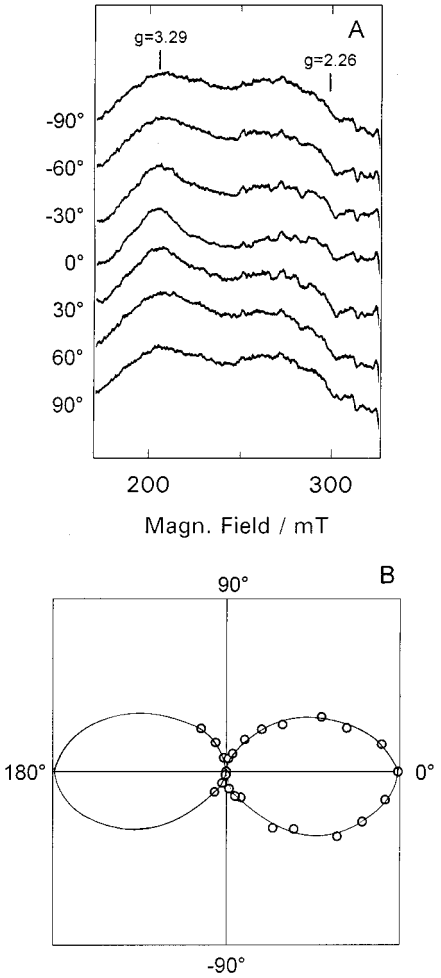

FIGURE 5: Orientation dependence of EPR signals of oxidized cyt c_2 cross-linked to the RC. (A) Spectra taken for a progressive rotation of the multilayers in the magnetic field. Angles are given between the plane of the multilayers and the direction of the magnetic field. (B) Polar plot for the amplitude of the $g_z = 3.29$ line at a given angle of the multilayers after subtraction of the signal at 90°. Conditions and instrument settings were as follows: temperature, 15 K; microwave power, 6.4 mW; frequency, 9.41 GHz; modulation amplitude, 2.1 mT; gain, 1×10^5.

DISCUSSION

Extent of RC Orientation in Polyacrylamide Gels. The RC were oriented for linear dichroism measurements by compression of polyacrylamide gels along one direction. This technique orients disk-shaped lipid vesicles or broken

membrane fragments which tend to align in a plane normal to the direction of compression (Abdourakhmanov *et al.*, 1979; Ganago *et al.*, 1980). In practice, the orientation is not perfect and for the analysis of linear dichroism data, the extent of sample orientation has to be determined independently. Therefore, we measured the light-induced polarized absorbance changes in the lower exciton band of the special pair P at 870 nm (Verméglio & Clayton, 1976; Rafferty & Clayton, 1979), the orientation of which is known with respect to the C_2 symmetry axis of the RC. The molecular *y*-directions for the two bacteriochlorophylls P_L and P_M intersect the membrane plane at an angle of approximately 18° (Ermler *et al.*, 1994). The Q_y transitions of P_L and P_M have been predicted from model calculations for the two BChl *b* of the *Rps. viridis* primary donor to deviate from the molecular *y*-axis by about 6° toward ring V, i.e., closer to the membrane plane (Scherer & Fischer, 1991). Even accounting for a small uncertainty in the polarization direction for the Q_y transitions of P_L and P_M or slight differences between the two individual monomer transitions in the *Rb. sphaeroides* RC used in this work, the antisymmetric linear combination of these two transitions should be polarized with high accuracy in a direction within the membrane plane. A similar polarization direction has been measured in previous optical linear dichroism and photoselection experiments (Verméglio & Clayton, 1976; Rafferty & Clayton, 1979) and low-temperature linear dichroism spectra (Breton, 1988). However, the determination of the polarization direction for an optical transition from its linear dichroism has its lowest precision at the extreme angles of 90° and 0° of θ. The extent of orientation of RC and RC−cyt c_2 complexes of $f = 0.48 \pm 0.03$ achieved by compression in the polyacrylamide gels is close to theoretical values that have been calculated as the limit for the extent of orientation that can be achieved by using this technique (Ganago *et al.*, 1980; van Amerongen & Struve, 1995).

Average Orientation of Cross-Linked cyt c_2. We determined the orientation of the two optical transitions contributing to the α-band of cyt c_2 with respect to the RC symmetry axis. These two nearly degenerate transitions are polarized within the heme plane (Eaton & Hochstrasser, 1967; Gouterman, 1978; Moore & Pettigrew, 1990). From the symmetries of the π- and π*-orbitals of the heme, they are expected to be polarized within the molecular *x*- and *y*-directions of the heme orthogonal to each other. However, the exact attribution to the molecular axes of the heme group is not known and may differ between individual cytochromes. Since the two transitions with maxima at 548.4 and 551.0 nm at room temperature differ clearly in their orientation (see Table 1), we tentatively identify the 548.4 nm transition which is found to be oriented more perpendicular to the membrane with the Q_x band, i.e., polarized within the ring II (exposed heme edge with the thiol bridge to Cys18) to ring IV (buried propionate) direction of the heme. This attribution places the solvent exposed ring II of the heme surrounded by positive surface charges toward the RC surface. A similar attribution has been proposed previously by Tiede (1987). The origin of the removal of the degeneracy of the porphyrin orbitals for some *c*-type cytochromes is not known and it may be due to small differences in the protein environment (Moore & Pettigrew, 1990). It is interesting to note that the attribution made here for cyt c_2, i.e., the blue-shifted transition lying in the ring II−ring IV direction, is that which is found for the heme c-556 in the tetraheme subunit of *Rps. viridis*. This is evident from comparison of the low-temperature linear dichroism spectrum of its split α-band (Verméglio *et al.*, 1989) and the X-ray structure of the RC from *Rps. viridis* (Deisenhofer & Michel, 1989).

The heme plane tilt angle for cross-linked RC−cyt c_2 complexes oriented in partially dried multilayers was determined independently by using EPR spectroscopy. The orientation dependence of the g_z signal of ferricyt c_2 at $g = 3.29$ shows that the g_z direction makes an angle of $0° \pm 10°$ with the membrane plane (Figure 5). Comparison of the minimum and maximum heights of the signal at $g = 3.29$ suggests that about 40−50% of the RC are oriented in the multilayer, whereas the remainder may be poorly ordered. Furthermore the analysis of heme orientation is rendered difficult due to broadening of the g_z signal relative to that of isolated ferricyt c_2. A variation in the position of the g_z signal of *c*-type cytochromes has also been observed as a function of pH (Brautigan *et al.*, 1977). Whereas the main g_y signal of isolated ferricyt c_2 is observed at $g = 2.06$, additional signals appear between $g = 2.4$ and 2.0 for the RC−cyt c_2 complexes. The most obvious signal at $g = 2.26$ was also observed for cross-linked RC−cyt c_2 complexes in solution. A similar variability in the g_y position of cyt c_2 was observed for partially dried multilayers of chromatophores from *Rb. sphaeroides* (J. Wachtveitl and W. Nitschke, personal communication). This suggests that these effects may be partially due to binding of the cyt c_2 to the RC as well as to the partial dehydration in the multilayers.

The resulting average orientation of cross-linked cyt c_2 relative to the RC which is suggested by the data from optical linear dichroism and EPR is depicted in Figure 6.

Orientation of cyt c_2 in Proximal Electron Transfer Complexes. The time-resolved linear dichroism measurements allow to detect possible differences in orientation between cytochromes c_2 differing in their functional properties, i.e., displaying different kinetic phases for the electron transfer to P^+. For cross-linked cyt c_2, the linear dichroism difference spectrum for the fast phase (Figure 2B, filled circles) is very similar to the average difference spectrum of cyt c_2 (Figure 2B, solid line). Therefore, the orientation of the (cross-linked) proximally bound cyt c_2 can be approximated by the orientation of the Q_x and Q_y transitions determined by the α-band line shape analysis for reduced cyt c_2 (Table 1).

Although the half-lives for the fast electron donation to P^+ from proximally bound cytochromes c_2 are identical for the cross-linked and the spontaneously formed complexes, the orientation of cyt c_2 is not the same in these two cases (compare Figure 2B and D). With the knowledge of the orientation of reduced cross-linked cyt c_2 within the proximal complex, we may interpret the differences between linear dichroism spectra of cyt c_2 in cross-linked and spontaneously formed proximal complexes (Figures 2B and D, filled circles) in terms of differences in cyt orientation. A simplified linear dichroism spectrum was calculated as the sum of the contributions of the Q_x and Q_y transitions of cross-linked cyt c_2 to the linear dichroism (see Figure 4 and Table 1) using eqs 3 and 1 (Figure 7A−C, solid lines). This serves as a reference representing the orientation given in Table 1 and Figure 6. For the sake of simplicity, the contribution of a third component was not considered in these simulations.

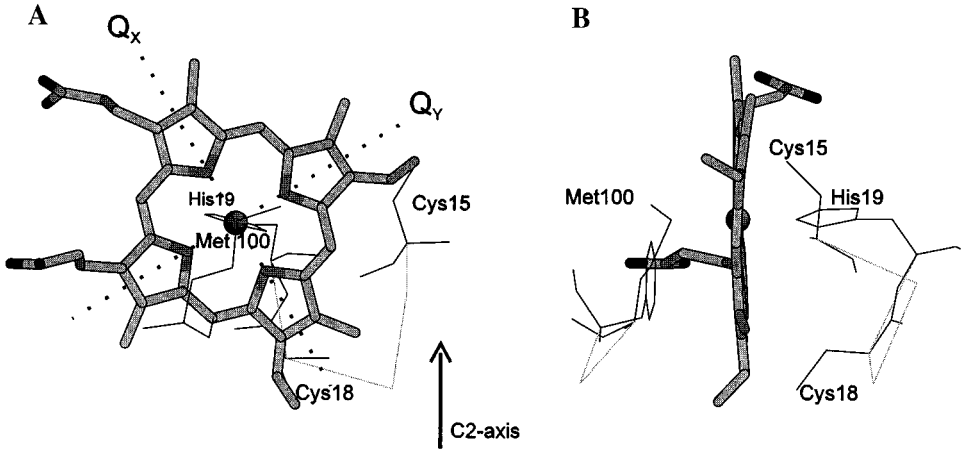

FIGURE 6: Schematic representation of the heme orientation of cross-linked cyt c_2 relative to the C_2 symmetry axis of the RC. Two views at 90° from each other. A few key residues of the cytochrome are indicated [coordinates from Axelrod *et al.* (1994); entry 1CXC, Protein Data Base, Brookhaven].

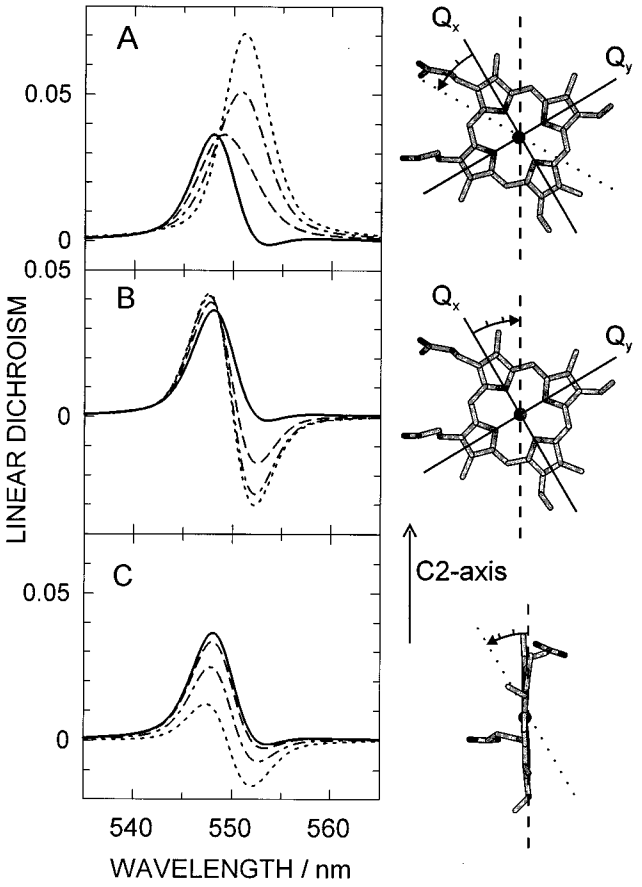

FIGURE 7: Simulation of the effect of variability in heme plane orientation on the linear dichroism spectrum for the α-band of cyt c_2. The average linear dichroism spectrum for cross-linked cyt c_2 is represented by the sum of the linear dichroism spectra of the Q_x and Q_y transitions as determined by the line shape analysis in Figure 4 (solid lines). The corresponding heme orientation serves as an initial configuration from which rotations of the cyt in three different directions (right panel) were analyzed with respect to their effect on the simulated linear dichroism spectrum. Each simulation proceeds in three consecutive steps of 10°. (A and B) The cyt is rotated around the heme plane normal in two opposite directions. (C) The cyt is rotated around an axis lying within the heme plane and parallel to the membrane plane, i.e., the heme is tilted toward the membrane plane.

Figure 7 (left panel) shows how the simulated linear dichroism spectrum of the cyt c_2 α-band changes upon rotations of the cyt in three different directions each proceeding in three successive steps of 10° as indicated on the right side of Figure 7. None of the rotations around the normal to the heme plane (Figure 7A and B) can account for the linear dichroism spectrum observed for cyt c_2 within the spontaneously formed proximal complex, i.e., a decrease in amplitude of the peak without a significant change of its shape (Figure 2D, filled circles). However, the simulated spectra in Figure 7C suggest that a tilting of the heme plane by about 20° may account for the lower amplitude of the linear dichroism spectrum for the fast oxidation of soluble cyt c_2 compared to cross-linked cyt c_2. This tilting results in orientations for Q_x of 38° and for Q_y of 59° relative to the symmetry axis. However, the linear dichroism data cannot distinguish between this possibility and an angular distribution of tilt angles, e.g., between 0° and 30°, with two or more conformations of the cyt that differ slightly in their orientation, but provide similar conditions for the fast electron transfer to P^+. This latter possibility can accommodate the observed orientation of cross-linked cyt c_2 assuming that in one of these possible conformations of the spontaneous complex competent in fast electron transfer cross-linking between the cyt and the RC may take place.

Non-Optimal Electron Transfer Complexes

Cross-Linked cyt c_2. Cross-linked cyt c_2 displaying the 60-μs phase shows an orientation similar to the average orientation of cross-linked cyt c_2 (Figure 2B, open squares and solid line, respectively). If significant, the slightly differing linear dichroism spectrum for the 60-μs phase may indicate (i) a rotation of the cyt by $<5°$ around the heme plane normal, with Q_x approaching the direction of the membrane normal (compare Figure 7B), or/and (ii) a tilting of the heme toward the membrane normal by $<10°$ (compare Figure 7C). However, such small differences in orientation are very unlikely to be the sole cause of the 80-fold slower electron transfer rate compared to the rate within the proximal complex.

Further differences in the conformation of the complex between the two kinetic phases may comprise a rotation of cyt c_2 around the membrane normal or a differing position of the cyt on the RC surface, which are not monitored in the linear dichroism measurements. In the preceding article we have shown that the two kinetic phases exhibit similar redox midpoint potentials and activation energies, rendering

unlikely effects of $\Delta G°$ or of the reorganization energy that could be responsible for the difference in electron transfer rate. Furthermore, the two phases have been found to involve a similar exclusive binding region on the RC surface (see preceding article).

The existence of two conformations of the complex having a nearly identical orientation of cyt c_2 can be rationalized by supposing that it is the interaction between the electrostatic dipole of cyt c_2 and negative surface charges on the RC that determines the orientation of the cyt relative to the membrane plane. The direction and strength of the dipole moment plays a major role in the efficiency of the bimolecular reactions of cyt *c* due to a pre-orientation of the cyt prior to the actual encounter with its reaction partner (Koppenol & Margoliash, 1982; Margoliash & Bosshard, 1983; Tiede *et al.*, 1993). Therefore, two different fits for the matching of the oppositely charged surfaces of the two proteins differing mainly in a rotation around the cyt c_2 dipole axis could provide locally optimized electrostatic interaction energies. As a result, a slightly different position of the exposed heme edge on the RC surface in these two conformations of the complex may lead to a difference in the heme to $(BChl)_2$ distance and in the rate of electron transfer. It is interesting to note that the two previous models for an electrostatically optimized complex proposed by Tiede and Chang (1988) or Adir *et al.* (1996) differ in a rotation of the cyt by ~90° around the RC symmetry axis.

An alternative explanation for the two conformations of the complex is suggested by the work from Adir *et al.* (1996). The authors have shown that electrostatic interaction between cyt c_2 and the RC orients the cyt similarly to its conformation in the co-crystal model, however, in a position farther away from the primary donor. They suggest that allowing side-chain reorientation would permit the more tightly bound complex as seen in the co-crystal. The two cross-linked populations having similar heme orientations observed in the present work could correspond to cyt molecules cross-linked before or after the induced fit of the side chains and penetration into the RC occurred.

Soluble cyt c_2. It is tempting to relate the 60-μs phase observed for cross-linked cyt c_2 to the analogous slower kinetic component of the P^+ reduction by soluble cyt c_2, the half-life of which in some studies had a first-order limit of 55−75 μs at high cyt concentrations (Long *et al.*, 1989; Tiede *et al.*, 1993; Wachtveitl *et al.*, 1993). In contrast to the slower phase of the P^+ reduction by soluble cyt c_2, the 60-μs phase of electron transfer from cross-linked cyt c_2 to P^+ is not decelerated by addition of glycerol (see preceding article) and is strongly dichroic (see Figure 2).

However, there are complications with the interpretation of this slower phase of P^+ reduction because several processes can be expected to contribute to this kinetic component, especially for the case of soluble cyt c_2:

(i) Bimolecular Reaction. For low cyt concentrations, the slower kinetic component reflects the second-order binding reaction. Under some conditions, it has been shown to be sufficient to account for the kinetics also at high cyt concentrations (Venturoli *et al.*, 1993; Tiede *et al.*, 1993).

(ii) Distal to Proximal Reorientation. When first-order behavior for this kinetic phase was observed, it was interpreted as due to a bound state of the cyt different from the proximal electron transfer complex. From its viscosity dependence, this phase was associated with a conversion from a distally bound cyt into the proximal configuration. However, the addition of glycerol may affect cyt binding and therefore the nature of the reaction may change due to the presence of glycerol.

(iii) Unbinding of Distal cyt c_2. Upon binding in a configuration that does not allow fast electron transfer, the cyt can be released and a new binding has to occur. At high cyt concentrations, the second order binding process would not limit the reaction and therefore the apparent first-order decay should monitor the off-rate of such a distal RC−cyt complex. In order to estimate the possible contribution of this pathway, we can calculate the off-rate for the proximal complex from its dissociation constant ($K_D = 3$ μM) and second-order binding rate constant [$k_{on} \approx 2 \times 10^9$ M^{-1} s^{-1}; see Venturoli *et al.* (1993) and Tiede *et al.* (1993)], yielding $k_{off} \approx 6 \times 10^3$ s^{-1}, corresponding to $t_{1/2} = 115$ μs. Here, we used the second order rate constant k_2 of P^+ reduction as a measure of k_{on}, assuming that the binding does not depend on the oxidation state of P. Since a distal complex may be less stable than the proximal one, the half-life for its decay may be even shorter. Thus, the half-life for the release of distally cyt c_2 could be close to the fastest observed first-order limits (55−75 μs) for the slower kinetic component and could also compete with an electron transfer process having a half-life of 60 μs.

(iv) Electron Transfer from Distally Bound cyt c_2. In the cross-linked complex, processes i−iii are blocked. Therefore, direct electron transfer from the distal cyt c_2 to P^+ becomes observable as the only possible reaction, a possible contribution of which in the case of spontaneously formed complexes might be difficult to identify.

The absence of linear dichroism in the absorbance changes of the intermediate kinetic phase for soluble cyt c_2 (Figure 2D) may suggest a higher variability in the orientation of the distally bound cyt c_2 than for the proximal complex. However, since the release of the oxidized cyt c_2 after the electron transfer is likely to occur within the time range of the slower kinetic phase (compare process iii, above), the linear dichroism for this kinetic phase may also be significantly decreased by the rebinding of reduced cyt c_2 into both the proximal and distal configuration.

Comparison with Previous Models for the RC−cyt c_2 Complex. In a previous linear dichroism study, Tiede (1987) arrived at a heme orientation of *Rb. sphaeroides* cyt c_2 bound to the RC having angles of 44.0° and 53.0° for the Q_x and Q_y transitions, respectively, and a heme plane tilt angle of 69.7°. The average orientation which we estimated for spontaneously bound cyt c_2 competent in fast electron transfer (see Figure 7C and discussion above) is close to that orientation (within ~10°). The small difference between the orientation in the previous study and that determined in our work here may be due to contributions from oriented cytochromes c_2 other than those in the proximal complex to the stationary linear dichroism spectrum in that study.

In the model proposed by Adir *et al.* (1996) for the structure of the RC−cyt c_2 complex in the co-crystals, the heme molecular *x*- and *y*-axes make angles of 9° and 88° with the RC symmetry axis, respectively (coordinates kindly provided by H. Axelrod and G. Feher) and the angle between the heme plane and the membrane is ~80°. Whereas this heme plane tilt angle is similar to that of 90° ± 10° and ~70°, which we determined for cross-linked and spontaneously bound cyt c_2, respectively, their cyt orientation differs

from those presented here by a rotation of ∼30° around the normal to the heme plane.

This discrepancy could be rationalized assuming that the variability in cyt orientation which we found for the cross-linked and spontaneously bound cyt c_2 in the proximal complexes being competent in fast electron transfer occurs to an even higher extent in the naturally formed complex. In the co-crystals, the non-physiological interaction between cyt c_2 and the H subunit of a symmetry-related RC may stabilize one unique structure out of a distribution of conformations occurring in solution. A variability in the complex conformation could also explain the low occupancy of 0.25 cyt c_2 per RC in the co-crystal. The existence of several configurations of the RC−cyt complex being almost equivalent in energy is also consistent with the mechanism proposed by Tiede *et al.* (1993) that the interaction of delocalized electrostatic domains is of primary importance for formation of docked complexes. Although by calculating the electrostatic interactions between cyt c_2 and the RC, Adir *et al.* (1996) identified one cyt position having the lowest electrostatic energy, these calculations indicated also a large number of cyt positions on subunit M having electrostatic energies within 25 mV, i.e., $\sim kT$ at room temperature, of the lowest energy structure.

CONCLUSIONS

The orientations of cyt c_2 in cross-linked and spontaneous, functional electron transfer complexes with the RC have been studied in detail. Comparison of the optical linear dichroism spectra at 295 and 10 K and complementary EPR measurements provide a reliable basis for the interpretation and quantitative analysis of linear dichroism data. The results allow a detailed model to be drawn for the orientations of cyt c_2 in electron transfer complexes with the RC. In cross-linked cyt c_2, the heme plane is parallel to the symmetry axis of the RC (0° ± 10°) and the Q_x and Q_y transitions which are assumed to be polarized within the heme plane make angles of 33° ± 6° and 56° ± 1°, respectively, with the symmetry axis. Using these results, the time-resolved linear dichroism of flash-induced absorption changes of cross-linked and non-cross-linked cyt c_2 were interpreted in terms of variations in the cyt orientation between functionally differing complexes. The proximal RC−cyt c_2 complex competent in fast electron transfer ($t_{1/2} \approx 0.7$ μs) showed a (dynamic or static) variation in cyt orientation with heme plane tilt angles between 0° and 20−30° relative to the membrane normal. It is suggested that in the naturally formed proximal RC−cyt c_2 complex the cyt orientation varies by ∼30° between configurations that are similarly stabilized.

The existence of two conformations of the cross-linked complex having nearly identical orientations of cyt c_2 suggests that its electrostatic dipole is optimally oriented in both complexes but that two different fits for the matching of the oppositely charged surfaces of the two proteins may provide locally optimized electrostatic interaction energies. These two conformations may differ (i) in a rotation around the cyt c_2 dipole axis and the exact position of the exposed heme edge on the RC surface or (ii) in the extent to which cyt c_2 has penetrated into the RC surface. A resulting difference of ∼3 Å in the heme to $(BChl)_2$ distance may account for the electron transfer rates differing by a factor of 80 between the two populations.

For the formation of the transient complex, a mechanism is proposed in which a pre-orientation of cyt c_2 relative to the membrane plane occurs by interaction of its strong electrostatic dipole with the negative surface charges of the RC. The optimal matching of the oppositely charged surfaces of the two proteins necessitates further rotation of the cyt around its dipole axis. Such a second step being energetically less well-defined than the first one may lead to non-optimal transient complexes resulting in a less efficient electron transfer reaction. Whereas in cross-linked complexes an electron transfer from such a distally bound cyt can be observed, for the spontaneous complex the dissociation of such a non-optimal complex and reformation in a bimolecular reaction is supposed to dominate the slower kinetic phase.

ACKNOWLEDGMENT

We thank Dr. Jacques Breton for instructions and stimulating discussions; Prof. George Feher and Dr. Herb Axelrod for providing coordinates of the cyt c_2−RC complex in the co-crystals; Drs. Josef Wachtveitl and Wolfgang Nitschke for the access to unpublished material and helpful discussions; and Aline Bluzat for the isolation of egg phosphatidylcholine. F.D. achnowledges support by a postdoctoral fellowship from the European Community.

REFERENCES

Abdourakhmanov, I. A., Ganago, A. O., Erokhin, K. E., Solov'ev, A. A., & Chugunov, V. A. (1979) *Biochim. Biophys. Acta 546*, 183−186.

Adir, N., Okamura, M. Y., & Feher, G. (1994) *Biophys. J. 66*, A127.

Adir, N., Axelrod, H. L., Beroza, P., Isaacson, R. A., Rongey, S. H., Okamura, M. Y., & Feher, G. (1996) *Biochemistry 35*, 2535−2547.

Allen, J. P., Feher, G., Yeates, T. O., Komiya, H., & Rees, D. C. (1987a) *Proc. Natl. Acad. Sci. U.S.A. 84*, 5730−5734.

Allen, J. P., Feher, G., Yeates, T. O., Komiya, H., & Rees, D. C. (1987b) *Proc. Natl. Acad. Sci. U.S.A. 84*, 6162−6166.

Aquino, A. J. A., Beroza, P., Beratan, D. N., & Onuchic, J. N. (1995) *Chem. Phys. 197*, 277−288.

Axelrod, H. L., Feher, G., Allen, J. P., Chirino, A. J., Day, M. W., Hsu, B. T., & Rees, D. C. (1994) *Acta Crystallogr. D50*, 596−602.

Blasie, J. K., Erecinska, M., Samuels, S., & Leigh, J. S. (1978) *Biochim. Biophys. Acta 501*, 33−52.

Brautigan, D. L., Feinberg, B. A., Hoffman, B. M., Margoliash, E., Peisach, J., & Blumberg, W. E. (1977) *J. Biol. Chem. 252*, 574−582.

Breton, J. (1985) *Biochim. Biophys. Acta 810*, 235−245.

Breton, J. (1988) in *NATO Advanced Research Workshop on the Structure of the Photosynthetic Bacterial Reaction Center: Structure and Dynamics* (Breton, J., & Verméglio, A., Eds.) NATO Advanced Science Institutes Series A443, pp 59−69, Plenum Press, New York.

Breton, J., Bylina, E. J., & Youvan, D. C. (1989) *Biochemistry 28*, 6423−6430.

Caffrey, M. S., & Cusanovich, M. A. (1994) *Biochim. Biophys. Acta 1187*, 277−288.

Chang, C.-H., El-Kabbani, O., Tiede, D. M., Norris, J., & Schiffer, M. (1991) *Biochemistry 30*, 5352−5360.

Chirino, A. J., Lous, E. J., Huber, M., Allen, J. P., Schenk, C. C., Paddock, M. L., Feher, G., & Rees, D. C. (1994) *Biochemistry 33*, 4584−4593.

Curry, W. B., Grabe, M. D., Kurnikov, I. V., Skourtis, S. S., Beratan, D. N., Regan, J. J., Aquino, A. J., Beroza, P., & Onuchic, J. N. (1995) *J. Bioenerg. Biomembr. 27*, 285−293.

Deisenhofer, J., & Michel, H. (1989) *EMBO J. 8*, 2149−2170.

Drepper, F., Dorlet, P., & Mathis, P. (1997) *Biochemistry 36*, 1418−1427.

Eaton, W. A., & Hochstrasser, R. M. (1967) *J. Chem. Phys. 46*, 2533−2539.
Ermler, U., Fritzsch, G., Buchanan, S. K., & Michel, H. (1994) *Structure 2*, 925−936.
Feher, G., & Okamura, M. Y. (1978) in *The Photosynthetic Bacteria* (Clayton, R. K., & Sistrom, W. R., Eds.) pp 349−386, Plenum Press, New York.
Ganago, A. O., Fok, M. V., Abdourakhmanov, I. A., Solov'ev, A. A., & Erokhin, K. E. (1980) *Mol. Biol. (Moscow) 14*, 381−386.
Gouterman, M. (1978) in *The Porphyrins* (Dolphin, D., Ed.) Vol. 3, pp 1−165, Academic, New York.
Hall, J., Zha, X., Durham, B., O'Brien, P., Vieira, B., Davis, D., Okamura, M. Y., & Millet, F. (1987a) *Biochemistry 26*, 4494−4500.
Hall, J., Zha, X., Yu, L., Yu, C. A., & Millet, F. (1987b) *Biochemistry 26*, 4501−4504.
Hofrichter, J., & Eaton, W. A. (1976) *Annu. Rev. Biophys. Bioeng. 5*, 511−560.
Koppenol, W. H., & Margoliash, E. (1982) *J. Biol. Chem. 257*, 4426−4437.
Long, J. E., Durham, B., Okamura, M., & Millet, F. (1989) *Biochemistry 28*, 6970−6974.
Mailer, C., & Taylor, C. P. S. (1972) *Can. J. Biochem. 50*, 1048−1055.
Margoliash, E., & Bosshard, H. R. (1983) *Trends Biochem. Sci. 8*, 312−320.
Mathis, P. (1994) *Biochim. Biophys. Acta 1187*, 177−180.
McLendon, G. (1991) *Struct. Bonding (Berlin) 75*, 159−174.
McLendon, G., & Hake, R. (1992) *Chem. Rev. 92*, 491−490.
Michel-Villaz, M., Saibil, H. R., & Chabre, M. (1979) *Proc. Natl. Acad. Sci. U.S.A. 76*, 4405−4408.
Moore, G. R., & Pettigrew, G. W. (1990) *Cytochromes C: Evolutionary, Structural, and Physicochemical Aspects*, Springer-Verlag, Berlin.
Moser, C. C., Page, C. C., Farid, R., & Dutton, P. L. (1995) *J. Bioenerg. Biomembr. 27*, 263−274.
Nabedryk, E., & Breton, J. (1981) *Biochim. Biophys. Acta 635*, 515−524.
Northrup, S. H., Boles, J. O., & Reynolds, J. C. L. (1987) *J. Phys. Chem. 91*, 5991−5998.
Okamura, M. Y., & Feher, G. (1983) *Biophys. J. 41*, 122a.
O'Reilly, J. E. (1973) *Biochim. Biophys. Acta 292*, 509−515.
Rafferty, C. N., & Clayton, R. K. (1979) *Biochim. Biophys. Acta 546*, 189−206.
Richard, P., Pitard, B., & Rigaud, J.-L. (1995) *J. Biol. Chem. 270*, 1−8.
Rongey, S. H., Juth, A. L., Feher, G., & Okamura, M. Y. (1994) *Biophys. J. 66*, A228.
Rothschild, K. J., & Clark, N. A. (1979) *Biophys. J. 25*, 473−488.
Scherer, P. O. J., & Fischer, S. F. (1991) in *The Chlorophylls* (Scheer, H., Ed.) pp 1079−1093, CRC Press, Boston.
Singleton, W. S., Gray, M. S., & White, J. L. (1965) *J. Am. Oil Chem. Soc. 42*, 53−57.
Taylor, C. P. S. (1977) *Biochim. Biophys. Acta 491*, 137−149.
Tiede, D. M. (1987) *Biochemistry 26*, 397−410.
Tiede, D. M., & Chang, C.-H. (1988) *Isr. J. Chem. 28*, 257−288.
Tiede, D. M., & Dutton, P. L. (1993) in *The Photosynthetic Reaction Center* (Deisenhofer, J., & Norris, J. R., Eds.) pp 257−288, Academic Press, New York.
Tiede, D. M., Vashishta, A.-C., & Gunner, M. R. (1993) *Biochemistry 32*, 4515−4531.
van Amerongen, H., & Struve, W. S. (1995) *Methods Enzymol. 246*, 259−283.
Venturoli, G., Mallardi, A., & Mathis, P. (1993) *Biochemistry 32*, 13245−13253.
Verméglio, A., & Clayton, R. K. (1976) *Biochim. Biophys. Acta 449*, 500−515.
Verméglio, A., Breton, J., Barouchi, Y., & Clayton, R. K. (1980) *Biochim. Biophys. Acta 593*, 299−311.
Verméglio, A., Richaud, P., & Breton, J. (1989) *FEBS Lett. 243*, 259−263.
Wachtveitl, J., Farchaus, J. W., Mathis, P., & Oesterhelt, D. (1993) *Biochemistry 32*, 10894−10904.

BI961351M